ORIENTAL JOURNAL OF CHEMISTRY
An International Open Access, Peer Reviewed Research Journal
www.orientjchem.org
ISSN: 0970-020 X
CODEN: OJCHEG
2026, Vol. 42, No.(1):
Pg. 146-154

Modification of Sawdust Biowaste using Chitosan Polymer and their Application for Congo Red Removal

ROMIT ANTIL[1] and ANIL K BERWAL[1]*

[1]*Centre of Excellence for Energy and Environmental Studies, Deenbandhu Chhotu Ram University of Science & Technology, Murthal, Sonipat 131039, HR, India.
*Corresponding author E-mail: romit.antil2@gmail.com

http://dx.doi.org/10.13005/ojc/420115

(Received: May 19, 2025; Accepted: July 19, 2025)

ABSTRACT

In the present study, an innovative application was proposed for the sawdust waste, which is an environment friendly material. For the remediation of Congo red dye, an adsorbent material made of zinc oxide, sawdust, and chitosan (CS) was synthesized. Variations in the following adsorption parameters were used to improve the adsorption tests: (i) pH (2.0–12.0), (ii) contact period (20 min–180 min), (iii) starting dye concentration (30–150 mg/L), (iv) adsorbent mass (10–80 mg), and (v) temperature $5^{O}C$–$30^{O}C$ in 100 mL of solution. Under various testing circumstances, the optimized adsorption study demonstrated that the synthesized adsorbent removed the dye from the aqueous medium. The study's primary results include the outstanding performance of the adsorbent material, which enabled maximal Congo red removal efficiency at 6.0 pH, 40 mg dose, 30 mg/L concentration with 100 min of contact time period, which is crucial for industrial procedures. Weak electrostatic forces cause the monolayer to adsorb, as seen by the removal's equilibrium isotherm. The sorption rate follows second-order pseudo kinetics. The ΔS^{O} and ΔH^{O} show that the reaction is endothermic, and negative ΔG^{O} values depicted that the adsorption is spontaneous. In addition to being materials made from trash, they may be reused more frequently, which aligns with the circular economy notion.

Keywords: Biowaste, Polymer, Congo red, Chitosan.

INTRODUCTION

A class of pollutants known as emerging contaminants has not yet been regularly monitored or adequately treated in wastewater treatment facilities, but has lately been found in water streams with use of advanced analytical tools. The absence of regulatory frameworks to regulate these pollutants' levels, in spite of health risks they bring to people and other living things when they build up in water bodies, is a significant worry. Along with the recently identified contaminants that belong to several categories of pesticides, flame retardants, personal care items, and medications, there are also legacy pollutants that have been there for a while, but worries about their potential risks are continuously growing.[1] The azo-dye Congo red (CR) is one of these pollutants. Over 70% of approximately one million tons of dyes produced annually worldwide are thought to be azo-dyes, of which 10–15% are discharged into

wastewater, resulting in wastewaters with high level of TDS, BOD, and COD.[2] Azo-dyes endanger both human life and the ecology by causing allergies, dermatitis, and mutation in humans alongwith blocking light transmission to living things that depend on photosynthesis.[3,4] In textile wastewater, the content of CR in particular has increased to around 60 ppm.[5] One of the main issues with organic contaminants in water is organic dyes. Congo red is one of the relevant organic pigments found in water. Because of its intricate aromatic structure, this secondary diazo dye is comparatively persistent and non-biodegradable. Congo red dissolves readily in water, making removal from polluted water challenging in a number of ways. It damages theskin, eye, respiratory system, and reproductive system and is poisonous and carcinogenic.[6]

The adsorption study's effectiveness, sludgefree action, ease of handling, and variety of adsorbent, the adsorption process is considered a good method for uptake of heavy metal ions from solution. Biochar is a widely used adsorbent due to its huge surface area and easy accessibility. Due to the high cost of commercial biochar, efforts were made to find a less expensive way to make biochar from waste biomass.[7] A thorough review of the literature shows that various adsorbents, such as activated carbon, chitosan, agricultural waste,polymeric compounds etc., were used to get rid of dyes. Sawdust, which contains cellulose, hemicellulose, and lignin, is one of the most abundant and lowest solid agricultural wastes that is now accessible.[8] Furthermore, the literature review makes it clear that altering the adsorbents surfaces enhances their ability to adsorb metal ions. Chitosan, a glucosamine biopolymer, has garnered a lot of interest in the removal of dyes and organic species due to its potent metal chelating capabilities and ease of application. By generating Schiff bases, the strong metal chelating capacity of the amino and hydroxyl groups of chitosan molecules enhances stability in acidic conditions.[9,10]

Congo red is anticipated to be adsorbed on the surface of zinc oxide due to its surface area, surface charge, and porosity. The current work aims to create and optimize the synthesis parameters in order to get the most appropriate and effective sawdust-chitosan based zinc oxide nanocomposite (NC), as the form, stability, and crystallinity of NC depend on the reaction variables. Chitosan on the zinc oxide surface may enhance Congo red adsorption even further. As a result, NC were created under a variety of artificial circumstances, and the resulting NC was developed as a novel adsorbent for the adsorption of Congo red.

MATERIALS AND METHODOLOGY

Materials

The sawdust waste from a neighboring sawmill. The dye stock solution was made using Congo red dye that was purchased from Aldrich Chemicals. Aldrich Chemicals chitosan analytical quality was utilized. The chemicals purchased from Merck India, including ethanol, sulfuric acid, sodium hydroxide, nitric acid, hydrogen peroxide, glutaraldehyde, and zinc nitrate. Double distilled water used for sample preparation of all solution. The pH solutions were maintained using a mixture of KCl and HCl for a pH range of 3.0, CH_3COONa and CH_3COOH for a pH range of 4.0 to 6.0, and NaOH and boric-acid for a pH range of 8.0 to 10.0.

SD is collected from a local sawmill and utilized as a precursor. Any impurities that could have stuck to the wood sawdust are removed with water. After drying for 24 h at 100°C in an oven, it is crushed and sieved. Biochar is made from SD via direct pyrolysis. The pyrolysis process is carried out in a muffle furnace. In a crucible with a cover, 20 g of SD is heated to 600°C for two hours in a muffle furnace then, allowed to cool to room temperature. It is subsequently pulverized using a mortar and pestle to produce biochar.[11] The chitosan-modified biochar was made by combining 2.0 g of chitosan with 360 milliliters of acetic acid, and then adding 6.0 g of the biochar to the mixture. To create a consistent suspension, the liquid was then agitated for 60 min with a stirrer. An 1800 mL NaOH solution was then filled dropwise with the biochar-chitosan homogeneous suspension, which was left there for 15 hours. Following around ten rounds of washing with DI water to remove any remaining unreacted NaOH, mixture was dried for 30 h at 110°C to produce in oven to produce BC-chitosan composites.[12,13]

Firstly, 4.0 g of Zinc Oxide added to a 1% CH_3COOH solution to create BC-Chitosan-ZnO composite. Next, 2.0 g of BC-chitosan was added

to the mixture. Following 60 min of intense magnetic stirring and sonication, 0.10N NaOH added to bring pH of solution down to 7.0, and it was then treated for two hours at 70–75°C. After that, the solution was dried for two hours at 60°C in an air oven.[14]

The SEM-EDS was used to examine the composite's morphological characteristics. XRD was used to determine the composite's crystalline structure. FTIR spectroscopy used to identify composite's basic functional group.

Congo red (CR), a model organic pollutant from the Merck Group, was used to analyze the adsorption models. A 1.0 L of distilled water was used to dissolve 1000 mg of MB in order to create the stock solution (1000 mg/L). The pH parameter of CR solution was adjusted to the anticipated values of 2.0, 4.0, 6,.0 8.0, 10.0 and 12.0 using 0.010M of NaOH and HCl solution. The container holding combination of sorbent particle and sorbate molecule was kept at 25°C in a temperature-controlled shaker-bath. The CR adsorption capacity qe was calculated using the following formula based on the residual CR concentration:

$$\text{Adsorption efficiency (\%)} = \frac{Ci - Cf}{Ci} * 100$$

$$\text{Adsorption capacity (qe)} = \frac{Ci - Cf}{m} *_{V}$$

Where, V is vol of the solution, m is amount of composite.

q_e and C_e, represent the adsorption capacity and the residual CR concentration when the adsorption goes to equilibrium.

RESULT AND DISCUSSION

SEM and EDS offer a powerful tool for examining the nanoparticle's topography and morphology. The nanocomposite's surface is rough and uneven, with a number of lumps that vary in diameter, as shown in Fig. 1(a)-1(b) SEM micrographs. Additionally, it is easy to recognize the numerous solid particles that came to the top. Nanocomposite component were found by Energy Dispersive X-ray spectroscopy (EDS). The elements oxygen (23.5%), carbon (59%), and zinc (11.9%) are present in the synthesized composite, according to the EDS spectra (Figure 1(c)).

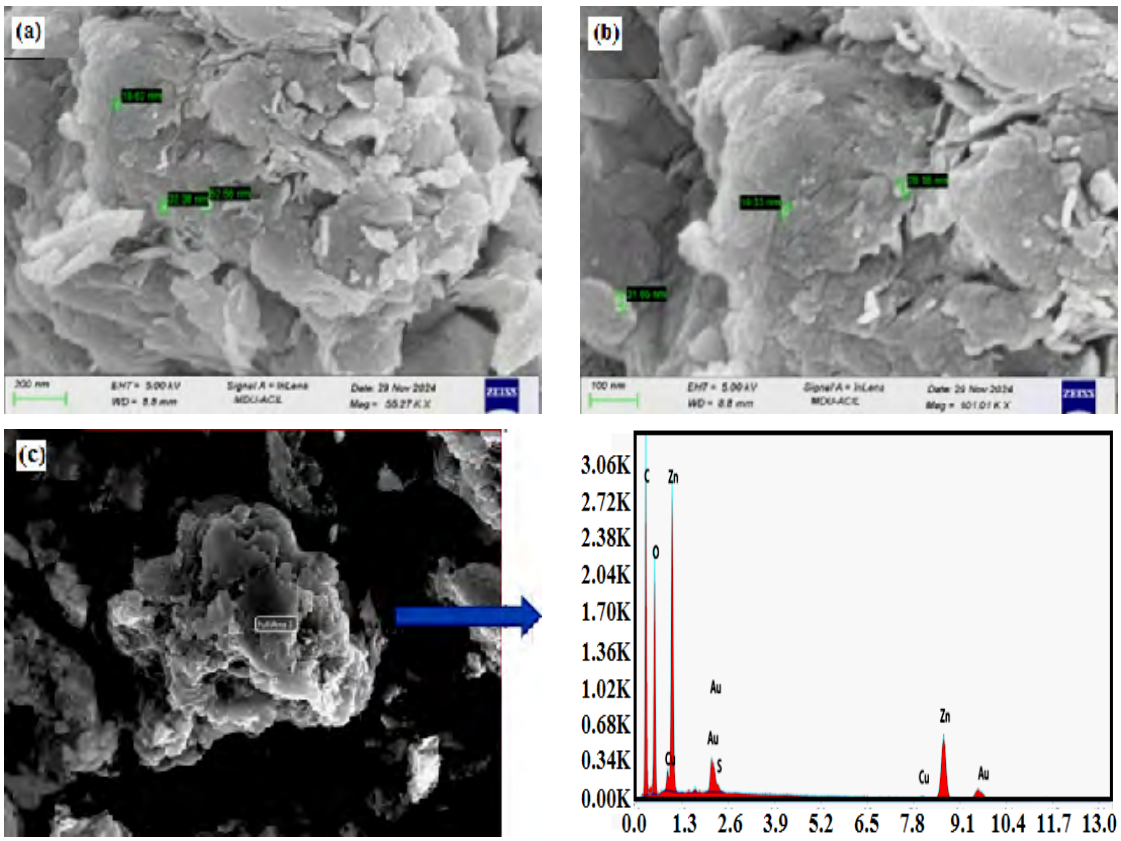

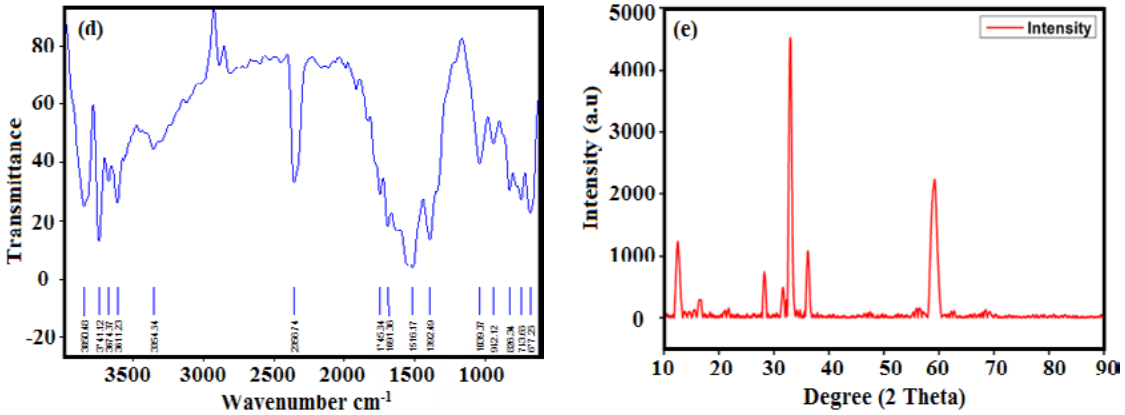

Fig. 1. SEM micrographs of synthesized nanocomposite (a-b); EDS of nanocomposite (c); FTIR spectrum (d); and XRD pattern of sawdust-chitosan based zinc nanocomposite (e)

The atomic and molecular bond vibrations of nanocomposite made from walnut shells utilizing the green synthesis technique were characterized by FTIR analysis. The existence of surface functional groups, which are crucial to the adsorption process, was demonstrated using it. By controlling the processes involved and increasing the adsorption capacity of solid adsorbents beyond their surface area, these functional groups significantly influence the behavior of adsorption. The existence of specific bindings connected to NPs is supported by the appearance of absorption bands in the acquired data. The emergence of discrete absorption bands supports and illustrates the presence of special bonds that are exclusive to NPs. The FTIR spectra of the produced nanocomposite was shown in Fig. 1(d). The detected spectra's C-H and -OH stretch vibrations of phenols and carboxylic acids are responsible for the IR peak located at 3851 cm^{-1} and 3743 cm^{-1}. The FTIR spectra bands at 3344 cm^{-1}, 2939 cm^{-1}, and 2357 cm^{-1} indicate the presence of alcohols, esters, carboxylic acids, and phenols, which are represented by the C-H, C=O, and -OH stretches. The IR peak at 1744 cm^{-1}, 1509 cm^{-1}, 1388 cm^{-1}, and 1035 cm^{-1} were ascribed to the presence of amine (N-H bend), aliphatic amine (C=O stretch), and carboxylic acid (C-H bend, C-N stretch). The possible existence of phenolic acids, carboxylic groups, alcohols, free hydroxyl, and amines is indicated by the C-H and N-H bends. The –OH bend was responsible for the other peaks, which were located at about 941 cm^{-1}, 825 cm^{-1}, and 656 cm^{-1}. According to the FTIR analysis, a number of phenolic acids, carboxylic acids, and amines were detected. Other amine (-NH_2) functional groups may be detected using the chitosan polymer. When the nanocomposite is being made, these functional groups may act as reducing and capping agents.[15,16]

The crystalline phase and content of the produced NC was examined using XRD. The NC XRD pattern is shown in the Fig. 1(e). The peaks at 2θ value of 31.9°, 34.5°, 36.4°, and 62.9° correspond to the crystal planes of (100), (002), (101) and (103), respectively, addition to matching JCPDS card no. 36–145. These planes are linked to a wurtzite structure with hexagonal phase of ZnO. The findings showed that ZnO hexagonal phase has been successfully immobilized on chitosan.

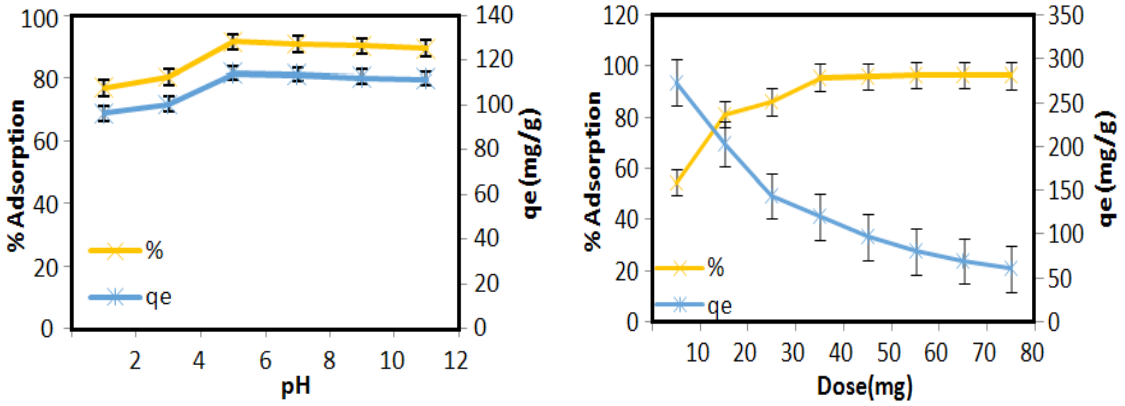

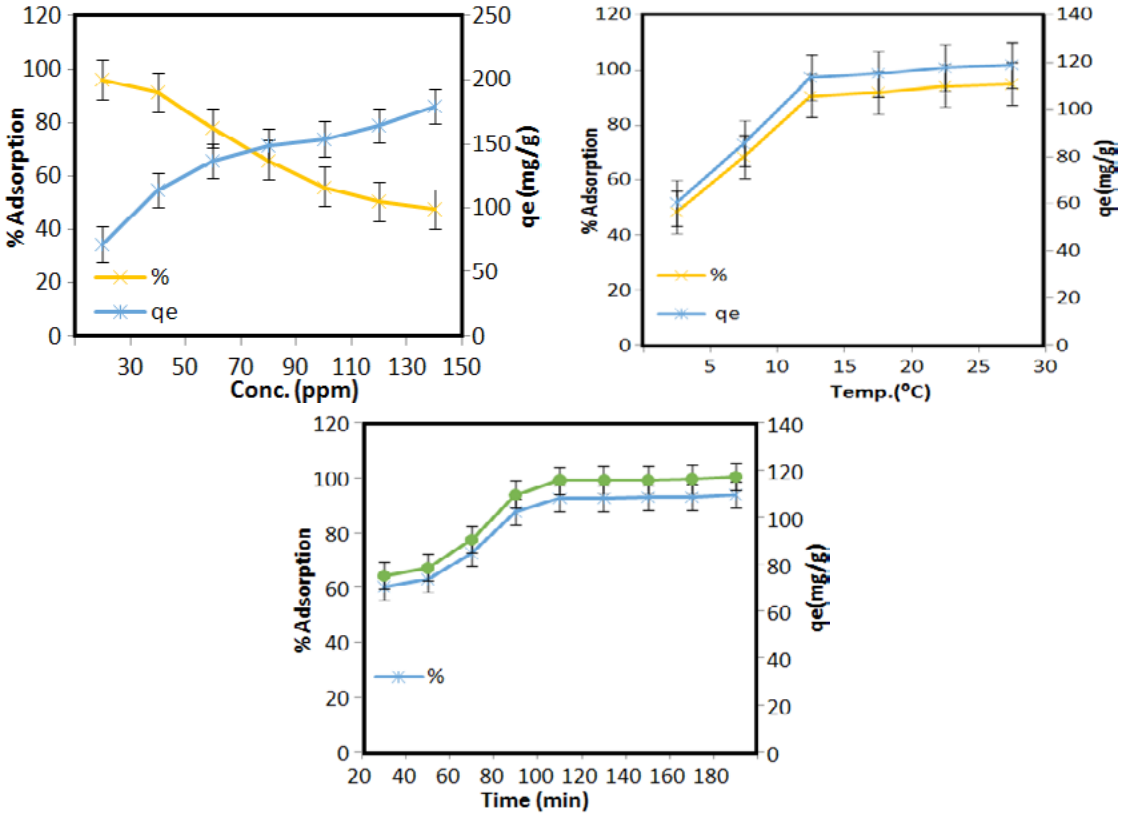

Fig. 2. Effect of pH; adsorbent dosage; initial dye concentration; temperature; and contact duration on Congo red dye adsorption

The solutionpH is a significant factor that influences surface-charge of adsorbents and CR molecule. With all other parameters held constant, the effect of solution pH on CR dye adsorption was examined in range of 2.0–12.0. The impact of pH on the dye's rate of adsorption onto the nanocomposite surface is depicted in Fig. 2. At pH 6.0 highest CR dye removal efficiency was 91.48% and maximum adsorption capacity was 114.35 mg g^{-1}. Although hybrid material charge was nearer to the -ve zeta-potential of -14.27mV and pHpzc 5.4, the cationic cellulose utilized as support maintained its positive charge and showed resistance properties. This is because the hybrid may adsorb at any pH because of the +ve charged zeta-potential of +3.65 mV that the quaternary ammonium groups on its surface.[17,18,19] However, partial +ve charge of the cellulose cause an adsorption ignition, allowing for a further rise in adsorption even in the presence of the oxide's negative characteristic. The potential for a $\pi-\pi$ stacking reaction between CR molecules to occur justifies it. The surface charge of the NC reduces its ability to attract additional molecules as the number of adsorbed layers grows, but the CR intermolecular connection persists. As NC contains carboxyl and amino groups, which are essential to CR adsorption, it exhibits favorable characteristics for CR adsorption. This adsorption results in electrostatic-attraction and a hydrogen-bond between adsorbent and CR, which creates an environment that is conducive to favorable adsorption capacity.[20,21] The adsorbent dosages varied from 10mg to 80mg with 6.0 pH, 50mg/L concentration at 25°C for 100 min, then after that the absorbance was measured. The absorbance decreased as the adsorbent dose rose 272.5 to 60.1mg/g (10-80mg) because there were more adsorption sites and more dye could be adsorbed (Fig. 2). The effect of concentration was measured by various dye concentrations (30–150 mg/L), at 6.0pH, 40mg dose at 25°C and absorbance of the solution was then measured. The proportion of dye removed reduced as dye concentration increased, which might be explained by restricted number of adsorbent sites accessible forsorption. The highest removal was at a concentration of 30 mg/L was 95.86mg/g.

The effect of temperature was studied at temperature from 5 to 30°Celsius. The absorbance of solution dropped as the temperature rose because the NC could adsorb more color. The dye solution (100mL) containing 30mg/L was maintained with 40mg of nanocomposite at various contact times (20–180minute). The absorbance was then evaluated; as the contact time increased, the dye solution's absorbance fell and the NC were able to adsorb more dye onto them. There was no discernible increase in adsorption after 100 min, which might be explained by the fact that there are fewer sites available for adsorption after a given amount of time.

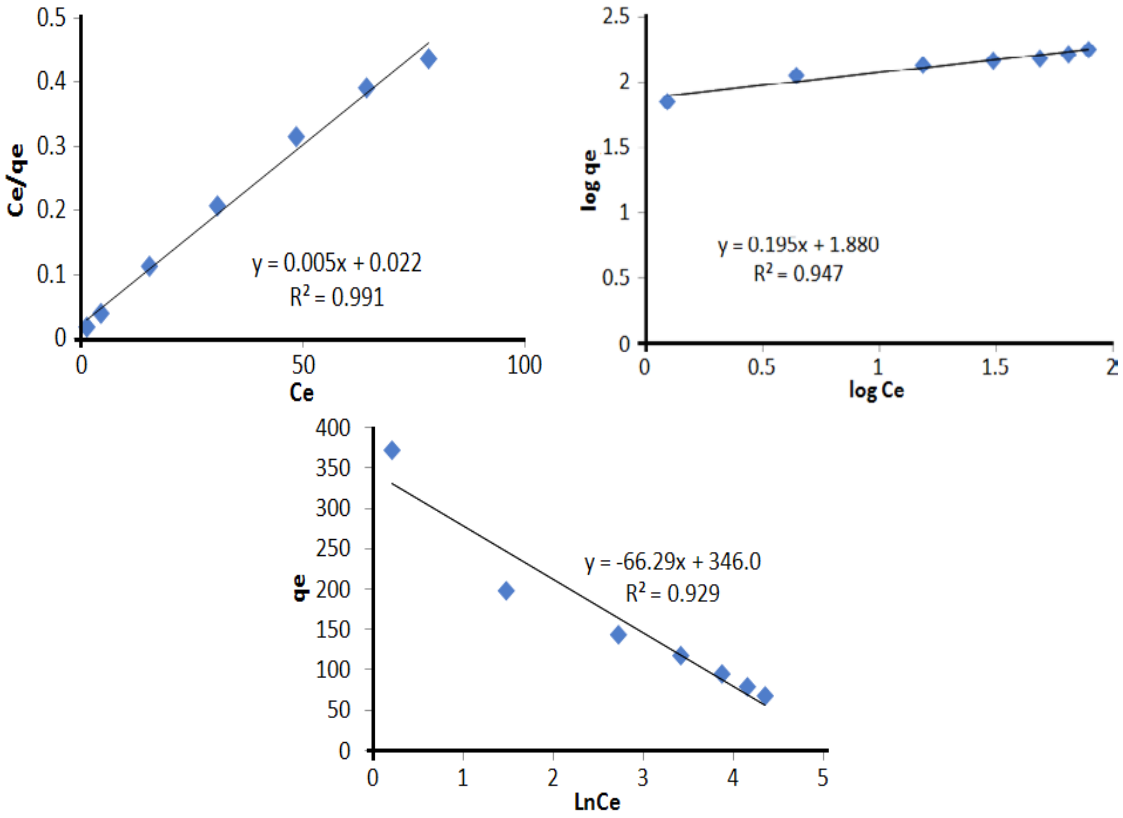

Fig. 3. Adsorption isotherms: Langmuir, Freundlich and Temkin isotherms

The adsorption isotherm is a crucial method to find out an adsorbent's maximum adsorption capacity. Adsorption isotherms are essential for comprehending adsorption mechanism for adsorbent. The adsorption capacity of the NC and the kind of adsorption process (chemical or physical) were ascertained using isotherm models. The Langmuir; Freundlich; and Temkin isotherms model in Fig. 3, respectively, were used to assess adsorption data and explain adsorption mechanism. The adsorptionparameterderived from Fig. 3 for several isotherm models are shown in Table 1. The monolayered coverage in model is used to calculate the adsorbent's maximum sorption capacity. The value of R_L and q_{max} were extracted from relationship between C_e/q_e and C_e (Fig. 3). NC has a maximum adsorption-capacity of 178.57 mg/g and b is 0.248. The separation factor (R_L) value, which is dimensionless and shows the shape of isotherm, is used to define the kind of adsorption process is 0.11. Langmuir isotherm model's regression coefficient (R^2) was determined to be 0.99.

On a heterogeneous surface, multilayer-adsorption is described by the Freundlich isotherm model. The exponential dispersal of energetic-active-center for multilayered sorption is also shown by this model. Plotting Log q_e versus Log C_e to be used to calculate the value of K_F and n. For CR adsorption, the K_F constant is 75.85 mg/g. The heterogeneity factors associated with adsorption strength, 1/n, indicates the adsorption intensity. Adsorption is considered negative when 1/n>1, and linear when 1/n=1, suggesting that the adsorbates do not interact. The

value of 1/n>1 indicated a weak sorption connection between the adsorbent and sorbate, whereas the value of 1/n<1 indicated a stronger adsorption-bond due to a high noncovalent-bond. Furthermore, it implies that adsorption is easy to do when 1/n falls between 0.1 and 0.5. The computed values of 1/n for dye adsorption was 0.195, suggesting that the CR dye and NC material have strong noncovalent interactions and that adsorption is simple to do. The Freundlich isotherm model's regression coefficient (R^2) was determined to be 0.94.

The indirect interactions between adsorbent and adsorbate are intended to be described using the Temkin isotherm model. It is predicated on the idea that as surface coverage rises, heat of adsorption (ΔH) of all molecule would drop linearly. Adsorbate solutions with moderate concentration ranges are most suited for this model. The value of AT as well as BT from graph (Fig. 3) depicting qe vs. Ln Ce were calculated. It was determined that the adsorption of CR dye had a BT value of 37.37 J/mol and AT 181.97. There was a regression value of 0.92.Consequently, Table 1 shows that Langmuir isotherm model has highest R^2 value. This suggests that Langmuir adsorption isotherm is followed by the CR adsorption process via NC.

Table 1: Isotherms, thermodynamics and kinetics

	Parameters	Values
Langmuir	q_{max}	178.57
	B	0.248
	R_L	0.11
	R^2	0.99
Freundlich	N	5.128
	K_f	75.85
	R^2	0.94
Temkin	AT	181.97
	R^2	0.79
	BT	37.37
Thermodynamics	ΔS°	0.315
	ΔH°	84.76
	ΔG° 278K	-2.82
	ΔG° 283K	-4.38
	ΔG° 288K	-5.96
	ΔG° 293K	-7.53
	ΔG° 298K	-9.11
	ΔG° 303K	-10.68
PFO	q_e	0.97
	K_1	4.58
	R^2	0.79
PSO	q_e	256.41
	K2	0.00064
	R^2	0.99

The properties of adsorption process, including chemical reaction, mass transfer, and calculating uptake-rate, are explained by adsorption kinetics. As shown in Fig. 4, kinetic of dye adsorption on NC were investigated using a number of kinetic model, including PFO andPSOas well as the mathematical equations that corresponded to each model. Table 1 displays the parameters for each model. Throughout the sorption process, it was found that the PSO model has a higher correlation coefficient than the first order model (R^2=0.999).

The adsorption process and the PSO kinetic model match well, suggesting that the quantity of solute adsorbed on adsorbent's surface and quantity of active sites influence sorption. The pseudo-second-order states that the active functional site on surface of sorbent have an inverse relationship with adsorption capacity. According to this hypothesis, valence forces—which serve as the rate-limiting stepare created when the CR and adsorbent share electrons. The equilibrium adsorption capacity (q_e=256.41 mg/g) obtained from PSO dynamic model is more in line with experimental value.It can be deduced that surface binding interactions (chemical adsorption) control the adsorption process since the bulk of dye is sorbed on adsorbentvia stronger noncovalent interaction.[22]

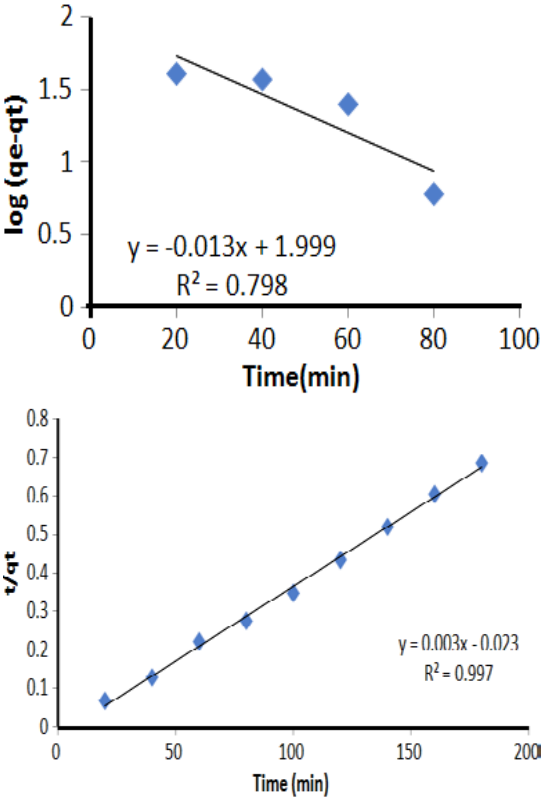

Fig. 4. PSO rate kinetics and PSO rate kinetic model

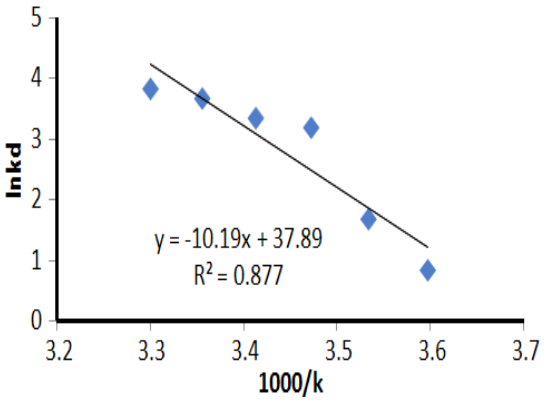

Fig. 5: Thermodynamic study

Figure 5 shows the linear connection between ln (K_d) and 1000/T(K) for adsorption process, while Table 1 provides information on the associated thermodynamic parameters. The adsorption of Congo red onto chitosan NC is an endothermic process, as indicated by positive values of ΔH° and ΔS°. This process is characterized by enhanced randomness at the solid-liquid interface, which favors adsorption. At the same time, the adsorption is confirmed to be spontaneous and thermodynamically beneficial by negative ΔG° values across temperature range.[23] Additionally, as temperature rises, ΔG° falls, suggesting better sorption effectiveness at higher temperatures, which is consistent with the patterns seen in Fig. 5. This pattern implies that by reducing the energy needed to achieve equilibrium, higher temperatures encourage more effective adsorption.

CONCLUSION

Chitosan nanocomposite was made for the purpose of removing CR dye in the present study. The closed arrangement of NP is revealed by surface morphology examination utilizing SEM with EDS analysis; XRD methods validate the significant peak for crystalline orientation with high strain. It has been confirmed through FTIR vibrational group analysis that the molecules have a bonding nature. For adsorption, the equilibrium duration was 100 minutes. Maximum adsorption occurs at a pH of 6.0. The temperature effect has been used to determine the thermodynamic parameter. The adsorption is spontaneous, as indicated by the negative ΔG° value, and it is an endothermic reaction, as indicated by the ΔH° and ΔS° values. The removal's equilibrium isotherm demonstrates the monolayer's sorption by weak electrostatic forces. However, the sorption rate adheres to pseudo second-order kinetics. For CR, the higher qmax value is 178.57 mg/g. All of these findings lend credence to our assessment that the NC is a viable option that functions as a matrix for dye removal activities.

ACKNOWLEDGMENT

The authors are thankful to DCRUST, Murthal.

Conflicts of Interest

The authors declare no conflicts of interest."

REFERENCES

1. Rout, P. R.; Zhang, T. C.; Bhunia, P.; & Surampalli, R. Y., *Science of the Total Environment.*, **2021**, *753*, 141990.
2. Wekoye, J. N.; Wanyonyi, W. C.; Wangila, P. T.;& Tonui, M. K., *Environmental Chemistry and Ecotoxicology.,* **2020**, *2*, 24-31.
3. Yadav, D.; Das, S.; Dhillayan, D.; Yadav, S.; & Bhukal, S., *Discover Agricul.,* **2025**, *3*(1), 1-18.
4. Gnanamoorthy, G.; Ali, D.; Yadav, V. K.; Dhinagaran, G.; Venkatachalam, K., & Narayanan, V., *Optical Materi.,* **2020**, *109*, 110353.
5. Farghal, H. H.; Nebsen, M.;& H., M. M., *Water.*, **2022**, *15*(4), 829.https://doi.org/10.3390/w15040829
6. Arab, C.; El Kurdi, R.;& Patra, D., *Chemosphere.*, **2021**, *276*, 130158.https://doi.org/10.1016/j.chemosphere.2021.130158
7. Yadav, S.; Bajar, S.; Hemraj, Rohilla, R.; Chhikara, S. K., & Dhankhar, R., *Sustainable Water Resources Management.,* **2023**, *9*(6), 174.
8. Buerge-Weirich, D.; Behra, P., & Sigg, L., *Aquatic Geochemistry.,* **2003**, *9*, 65-85.
9. Süry, P., *Corrosion Sci.,* **1976**, *16*(12), 879-901.
10. Ewecharoen, A.; Thiravetyan, P.; Wendel, E., & Bertagnolli, H., *Journal of hazardous materials.*, **2009**, *171*(1-3), 335-339.
11. Roy, H.; Islam, M. S.; Arifin, M. T.;& Firoz, S. H., *Sustainability.,* **2021**, *14*(21), 14571. https://doi.org/10.3390/su142114571
12. Yadav, S.; Yadav, A.; Goyal, G.; Dhawan, M.; Kumar, V.; Yadav, A., & Chhikara, S. K., *Orient. J. Chem.*, **2024**, *40*(1).
13. Mehmood, S.; Ahmed, W.; Ikram, M.; Imtiaz, M.; Mahmood, S.; Tu, S., & Chen, D., *Plants.*, **2020**, *9*(9), 1173.

14. Roy, H.; Islam, M. S.; Arifin, M. T.;& Firoz, S. H., *Environmental Nanotechnology, Monitoring & Management*., **2022**, *18*, 100752.
15. Muzyka, R.; Kwoka, M.; Smłowski, Ł.; Díez, N., & Gryglewicz, G., *New Carbon Materials*., **2017**, *32*(1), 15-20.
16. Al-Ghouti, M. A.; Sayma, J.; Munira, N.; Mohamed, D.; Da'na, D. A.; Qiblawey, H., & Alkhouzaam, A., *Environmental Technology & Innovation*., **2022**, *27*, 102525.https://doi.org/10.1016/j.eti.2022.102525
17. Yadav, S.; Rohilla, R., & Chhikara, S. K., Proceedings of the National Academy of Sciences, India Section B: *Biological Sciences*., **2024**, 1-9.
18. Yadav, S.; Dhawan, M.; Kumar, V.; Dalal, J.; Pandey, R.; Sehrawat, N., & Chhikara, S. K., *Discover Materials*., **2025**, *5*(1), 1-18.
19. Zyoud, A.; Zyoud, A. H; Zyoud, S. H.; Nassar, H.; Zyoud, S. H.; Qamhieh, N., & Hilal, H. S., *Environmental Science and Pollution Research*., **2023**, *30*(26), 68435-68449.
20. Jagusiak, A.; Piekarska, B.; Chłopaś, K., & Bielaśska, E., Self-Assembled Molecules–New Kind of Protein Ligands., **2018**, 121.
21. Tolosa, G. R.; Gomes, A. S.; Leal, M. V. G.; De Oliveira Setti, G.; Dognani, G., & Job, A. E., *International Journal of Biological Macromolecules*., **2024**, *277*, 134063.https://doi.org/10.1016/j.ijbiomac.2024.134063
22. Kayalvizhi, K.; Alhaji, N.; Saravanakkumar, D.; Mohamed, S. B.; Kaviyarasu, K.; Ayeshamariam, A.;& Elshikh, M. S., *Environmental Research*., **2021**, *203*, 111814. https://doi.org/10.1016/j.envres.2021.111814
23. Makhlouf, M. R.; Bendjaballah, M.; Boukerche, I.; Kouadri, I.; Hamidoud, S.; Benhamza, M. E. H., & Hammi, H., *Biomass Conversion and Biorefinery*., **2024**, 1-16.